

Nucleation of magnetic skyrmions at a notch

Maria N. Potkina^{1,b}, Igor S. Lobanov^{2,b}¹Infochemistry Scientific Center, ITMO University, St. Petersburg, Russia²Faculty of Physics, ITMO University, St. Petersburg, Russia^apotkina.maria@yandex.ru, ^blobanov.igor@gmail.com

Corresponding author: M. N. Potkina, potkina.maria@yandex.ru

PACS 82.20.Pm, 34.10.+x, 75.40.Mg

ABSTRACT Magnetic skyrmions are considered promising candidates for coding bits of information in racetrack memory devices. Information recording in such devices is assumed to occur by creating skyrmions. This work is devoted to finding solutions to make this process as energy-efficient as possible. One of the factors influencing the creation of skyrmions is the geometry of the track on which recording takes place. We study the influence of the shape and size of track boundary notches on the energy barriers of skyrmion nucleation. We show that skyrmions generation is facilitated by the presence of irregularities at the track boundary and the best solution is a deep narrow notch. On the other hand the skyrmion nucleation rate is smaller for smooth boundaries and skyrmions generation can be suppressed by their interaction with the track boundary, if notch size is smaller than the skyrmion radius. These results can be used in development of future memory devices based on skyrmions.

KEYWORDS transition state theory, topological magnetic solitons, nucleation, collapse, lifetime.

ACKNOWLEDGEMENTS MNP thank Y.M. Beltukov for useful discussions. The study was supported by the Russian Science Foundation grant No. 22-72-00059, <https://rscf.ru/en/project/22-72-00059/>. Priority 2030 is acknowledged for infrastructure support.

FOR CITATION Potkina M.N., Lobanov I.S. Nucleation of magnetic skyrmions at a notch. *Nanosystems: Phys. Chem. Math.*, 2024, **15** (2), 192–200.

1. Introduction

Magnetic racetrack memory is a perspective device for data storage proposed in 2008 by Parkin [1]. Currently large companies such as IBM are close to practical implementation of the devices, which requires to overcome some technical problems [2, 3]. Initial racetrack device was supposed to use domain wall (DW) as information carrier [1], but further research suggests that magnetic skyrmion (Sk) can be a better information carrier [3, 4]. In particular, Sk has smaller chances to pin to impurities than DW, hence energy consumption of Sk based devices is smaller [5–7], moreover Sk velocity can even increase due to interaction with impurities [8]. Function of Sk racetrack memory device consists of creation of Sk on the track (writing bit), moving Sk along the track (register shift), detection of Sk (reading) and annihilation of Sk (erasing). The material that the track is made of should both provide lifetime of Sk of decades at room temperature to be a reliable data storage, and Sk creation and annihilation should be energy efficient. Skyrmions stable at room temperature was found in ultrathin Pt/Co/MgO nanostructures [9]. Stability of Sk in Fe monolayer on an Ir(111) substrate was demonstrated in [10], and is theoretically predicted in [11, 12]. Creation of Sk can be achieved by several means, among which local heating using laser irradiation [13], applying local magnetic field [14] or by injection of current [15, 16]. The Sk generation can be facilitated by geometry of the system [17]. In particular, Sk tends to easier appear on the impurities [7, 18–21] as a result certain impurities can be used for Sk generation provided means to remove Sk from such an impurity, e.g. spin-polarized current can be applied. In the article we focus on creation of Sk by employing a notch, which represents the nonmagnetic impurity located at the track boundary. In [22] we have demonstrated that Sk generation rate due to thermal perturbations is much smaller at the boundary than inside the track. Below we show that the Sk generation at a side of the track can be significantly improved by creating a notch. This situation turns out to be more complicated for analysis, than the case of isolated impurity, because the interaction of Sk occurs not only with the impurity, but also with the boundary of the track.

An efficient generator of Sk should have the following properties: it should not create Sk in waiting mode and create Sk in robust manner under applied control. Nucleation of magnetic Sk on the track with a notch was investigated experimentally [23–26] and theoretically [27–32]. Despite the fact that the works [23–32] studied systems with different magnetic characteristics, geometries and external conditions, it was shown in all cases that notches may serve as a generator of skyrmions. However, these studies considered only one or several notches with fixed geometry, which is not enough for revealing the effect of notch design on Sk nucleation. In this work we systematically investigate this question

by making calculations of minimum energy pathes (MEPs) and energy barriers for skyrmion nucleation at notches of various geometry.

The notches can also be used to solve another problem with positioning of Sk on the track. While Sk can be moved by spin-polarized current [16, 33], electric current [34], or by voltage [35], small variation in the material parameters or in local current can lead to unexpected position of Sk and failure of the read operation. The problem can be solved by creating potentials wells, where Sk will slide to, when the spin transfer current is off. One way to create the well is to make a set of notches on the track [30, 36, 37]. Except for this purpose, at the same time, the notches can undesirably create and destroy Sk, therefore it is important to have design of the notches that resists to these processes. This issue will be analyzed in this work.

In this article we study skyrmion nucleation energy barrier on the notch in a magnetic track. For a fixed film parameters we study round and triangle notches for wide range of angles and radii. We show that Sk generation activation barrier depends on small size features such as single-atom steps on the boundary shape, medium size features such as notch curvature and on the distance from the notch to the global track boundary. Below we provide estimates for all the contributions.

2. Simulated system

We model a track for the movement of skyrmions in the racetrack memory [3]. The system is described by the atomistic generalized Heisenberg model with the energy

$$E = -J \sum_{\langle i,j \rangle} \mathbf{S}_i \cdot \mathbf{S}_j - \sum_{\langle i,j \rangle} \mathbf{D}_{ij} \cdot (\mathbf{S}_i \times \mathbf{S}_j) - \mu \sum_i \mathbf{B} \cdot \mathbf{S}_i - K \sum_i (S_i^z)^2, \quad (1)$$

where \mathbf{S}_i is a three-dimensional vector of unit length in the direction of the magnetic moment of a spin i of a two-dimensional crystal lattice. The first term describes the Heisenberg exchange with the parameter J for the magnetic moments of the nearest neighbors, the second term takes into account the Dzyaloshinskii-Moriya interaction (DMI) with the vector \mathbf{D}_{ij} lying in the plane of the track perpendicular to the vector connecting the spins i and j . The third and fourth terms correspond to the interaction with the external magnetic field and to the contribution of magnetic anisotropy with an easy axis along the z-axis perpendicular to the track plane. The spins magnetic moment μ , external field \mathbf{B} and anisotropy parameters K are assumed to be the same for all atoms. The summation $\langle i, j \rangle$ in (1) runs over all pairs of nearest neighbor atoms.

We studied Neel-type skyrmions on triangular lattice with the lattice constant $a = 2.7 \text{ \AA}$ and parameters $K = 0.49 \text{ meV}$, $|\mathbf{D}_{ij}| = 2.24 \text{ meV}$, $J = 7 \text{ meV}$, $\mu = 3\mu_B$, which corresponds to the Pd/Fe bilayer on the Ir(111) substrate [12]. This system maintains skyrmions of radius $3.95a$, defined as distance from skyrmion center to the ring $S^z = 0$. All calculations were carried out with the magnetic field value $|\mathbf{B}| = 3.75 \text{ T}$. Ground state for the selected parameters is ferromagnetic homogeneous everywhere except for boundary of the track where magnetic moments are twisted due to uncompensated DMI. For the considered parameters skyrmions are metastable states with energy 43.81 meV above ferromagnetic state. We are considering a part of the track, with the x-axis oriented along the track, and the y-axis oriented across it. Periodic boundary conditions are set along the track and the free boundary conditions are imposed on the track boundary. We simulated lattice of size $N_l \times N_w$ spins, with the first lattice vector coinciding with x-axis, that is we simulate track of length $N_l a$ and width $N_w b$, where $b = \sqrt{3}a/2$. We take the width N_w as $60 \div 90$ atomic rows, which was chosen large enough to make influence of boundaries negligible for isolated Sk at the central part of the simulated domain. N_l was chosen equal to N_w . Below we fix the coordinate system in such a way that spin (i, j) has the coordinates:

$$\frac{x}{a} = i + j \cos \frac{\pi}{3} + \frac{1 - N_l}{2}, \quad \frac{y}{a} = j \sin \frac{\pi}{3} + (1 - N_w) \sin \frac{\pi}{3}.$$

In the article we focus on generation of skyrmions due to boundary effects. The geometry of the magnetic film is taken into account by excluding spins belonging to the notch from the sums in (1). Due to discrete nature of the lattice, small variations in the geometry may lead to significant change in the number of spins belonging to the film, which, as will be shown below, affects Sk generation energy barrier. The notch is created by removing some spins from the track near its upper boundary. We consider two types of notches. The *round notch* is created by removing spins belonging to a circle:

$$x^2 + (y - Db)^2 \leq (Ra)^2,$$

where Ra is radius of curvature of the notch and Db is the distance from the circle center to the upper track side. We also remove the strip connecting the track boundary and the circle, see Fig. 2:

$$|x| < Ra \quad \text{and} \quad y > -Db.$$

Total penetration depth of the notch is $Ra + Db$. Large values of D are used to separate effect of interaction with the track boundary and with interaction with the notch.

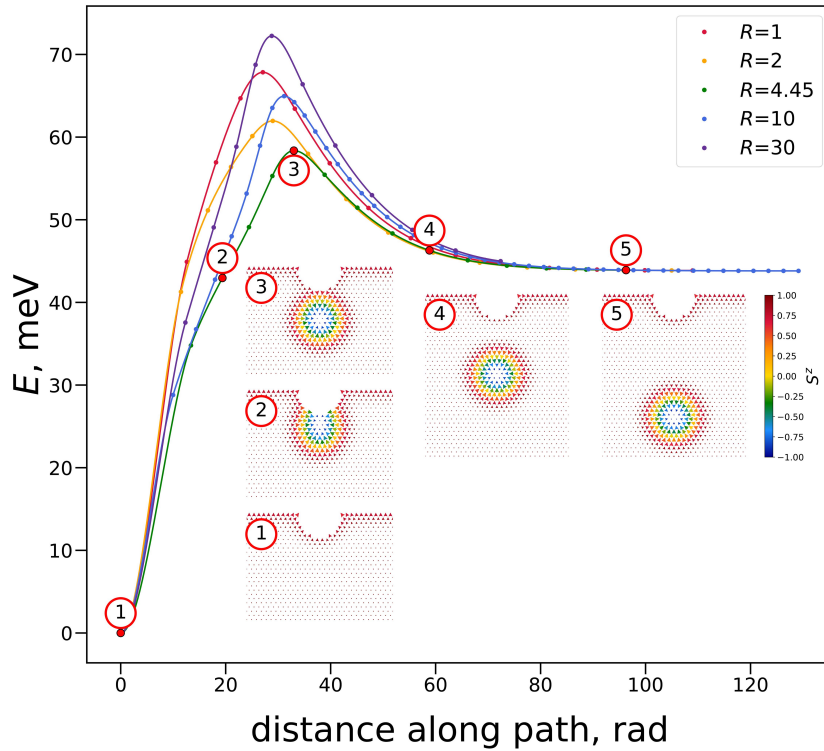


FIG. 1. MEPs for the nucleation of a skyrmion at round notch of various radius. The insets show magnetic configurations along the MEPs for $R = 4.45$. States 1 and 5 correspond to minima, state 3 corresponds to saddle point. The color in insets indicates the value of the out-of-plane component of the magnetic moments.

We also study *triangular notch*, where inner part of an angle is removed:

$$\left| \frac{x}{y+D} \right| < \tan \frac{\alpha}{2} \quad \text{and} \quad y > -Db,$$

see Fig. 6. The penetration depth in this case is D . Both notches are symmetric with respect to the line $x = 0$.

To estimate activation barriers for skyrmion nucleation we computed MEP, that is a continuous line in the phase space connecting initial and final state of magnetic texture such that each point of the line corresponds to the minimum of energy in the hyperplane orthogonal to the path at the point. In practice MEP is approximated by its discretization defined by several states of magnetization vectors (called images) computed numerically. In our computations we take $15 \div 50$ images along every path and employed string method for numerical optimization of MEP [38]. For all the paths the initial state was ferromagnetic and final state corresponds to the relaxed isolated skyrmion completely separated from the track boundary. To obtain MEP for skyrmion creation on the boundary, a reasonable initial approximation should be taken. In our study every image of the initial path contains a single copy of the equilibrium skyrmion with the center at $x = 0$ and $y = -30bl$, where l is the coordinate of reaction, $0 \leq l \leq 1$. The copy of Sk in the first image is centered at $(0, 0)$ and therefore extends beyond the track. The image is relaxed to the FM state during the MEP optimization.

3. Results

Round notch. We first studied the nucleation of skyrmions on the track with a semicircular notch centered on its boundary, see the notch shape in the insets of Fig. 1. Calculations of minimum energy paths were carried out for various radii of the notches, Fig. 1 shows the paths for the radii $R = 1, 2, 4.45, 10, 30$. As can be seen, the energy of the saddle point relative to the initial state without a skyrmion, that is, the barrier to nucleation, has a non-monotonic dependence on the notch radius. The insets in Fig. 1 show the magnetic configurations along the MEP for skyrmion nucleation at a notch radius of $R = 4.45$. Initial state 1 corresponds to the ground state having no skyrmions. Then the spins at the bottom of the notch begin to rotate so that a skyrmion is formed attached to the notch (inset 2). The maximum energy along the path corresponds to the state when the skyrmion core is fully formed and the boundaries of the skyrmion and the notch are in contact (inset 3). After passing the transition state the SK separates from the notch and moves away from it (insets 4 and 5).

We carried out calculations of the MEP for radii in the range from 1 to 30 with a step of 0.05 and obtained the dependence of the nucleation barriers on the radii of the notches, shown in Fig. 2 in blue. The energy barrier as the function of the notch radius oscillates with the period close to the lattice constant due to the discrete nature of the crystal lattice. The oscillations in most cases are associated with the appearance of a new series of vacancies with increasing notch size. The correlation between the number of removing atoms in the bottom row of the notch and the jumps in the barrier may be observed in Fig. 3a, which shows part of the dependence for the radius in Fig. 2a in the range from 13 to 14. Local maxima of the $\Delta E(R)$ dependence correspond to the maximum number of vacancies in the bottom row of notch, for example nine vacancies at $R = 13.85$, Fig. 3b, and local minima correspond to the appearance of a new row of vacancies with increasing radius, as for example in this case of $R = 13.9$ a new lower row of two atoms appeared (Fig. 3c).

When the radius of the notch tends to infinity, its boundary near the site of skyrmion nucleation tends to a straight boundary. Therefore, the barrier for skyrmion formation at the notch asymptotically tends to a constant value equal to the barrier for formation through the straight track boundary, $E_0 = 75.62$ meV, shown by green dashed line in Fig. 2a. Similar behavior is observed for the lower envelope, but in this case the notch boundary becomes similar to a flat boundary with the presence of one vacancy on it. The extreme point on the left on the blue graph corresponds to the situation of one vacancy on a straight boundary. The barrier in this case, according to our calculations, is $E_1 = 72.67$ meV, shown by purple dashed line.

To approximate the envelopes of the dependence of the barrier on the radius for $R > 16$, we used functions of the form $E_0 - p_0/R$ and $E_1 - p_1/R$ with parameters p_0 and p_1 , assuming the notch curvature is a perturbation parameter for

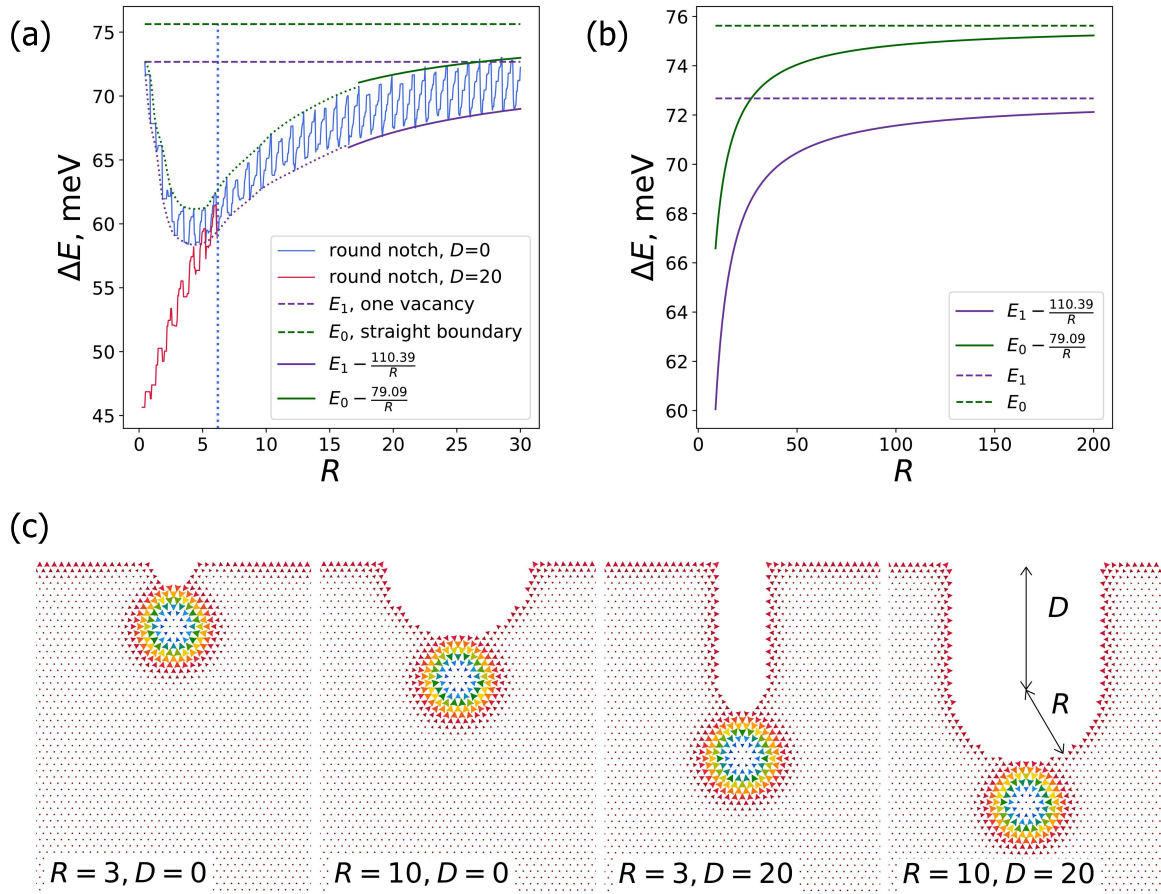


FIG. 2. (a) Energy barrier for skyrmion nucleation at the semicircular notch and round notch with depth $D = 20$ as a function of radius of notch. The vertical dotted line shows the radius value above which the barrier for nucleation at the semicircular notch and at the deep notch differ by less than 1%. Solid lines show approximations of envelopes of function of energy barrier for highest radii. Dashed lines shows asymptotics for upper and lower envelopes. (b) Approximations of envelopes and their asymptotics shown at larger interval of radius. (c) Transition state configurations for skyrmion nucleation at the boundary round notch with radius $R = 3$ and $R = 10$, and at deep round notch with depth $D = 20$ and radius $R = 3$ and $R = 10$.

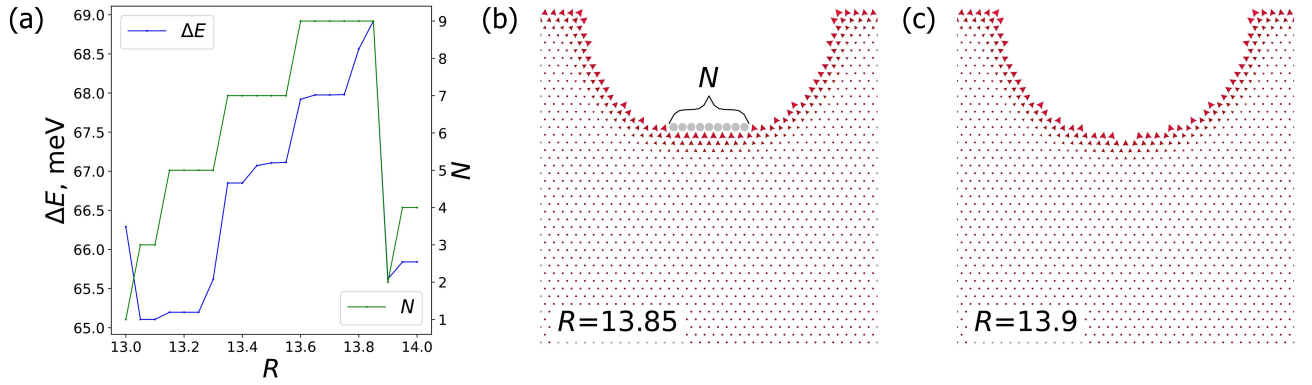


FIG. 3. (a) Energy barrier for skyrmion nucleation at the round notch and number of vacancies in the bottom row of notch as a function of radius of notch for $13 \leq R \leq 14$. Configuration of notch for radius $R = 13.85$ with exclusion of 9 atoms (b) and for radius $R = 13.9$ with exclusion of 2 atoms in the bottom row of the notch (c).

energy barrier of Sk creation on the flat boundary. Our fitting predicts the following interval of activation energy values for large R :

$$E_1 - 110 \text{ meV} \cdot R^{-1} \leq \Delta E \leq E_0 - 79 \text{ meV} \cdot R^{-1}.$$

The graph in Fig. 2b shows the envelopes and their asymptotic behavior over a larger range of radii. It allows to predict the approximate range of the barrier of skyrmion nucleation for specific value of notch radius.

As the radius decreases, the distance from the partially instantiated Sk at the transition state to the straight boundary decreases and it begins to influence the barrier. To decouple this effect from the influence of the curvature of the notch, we calculated the dependence of the barrier on the depth of the notch for the smallest Sk radius, Fig. 4a, that is the notch in the case is a chain of vacancies of one atom thick. We will further call a notch of this shape a needle. Fig. 4b and c show the saddle points for skyrmion nucleation for depths of 5 and 19. Note that the configurations differ: in the first case it has the shape of a drop, and in the second it has the shape of circle. This is because, as can be seen from Fig. 5, with an increase in D , an intermediate minimum (inset 3) and a second maximum (inset 4) appear on the MEP, which becomes dominant. This process is similar to the process of nucleation of Sk on impurities, which we studied earlier [7]. It also occurred in two stages, first the creation of a skyrmion attached to the impurity, then its separation from the impurity. As it is seen in Fig. 4a, the proximity of a flat boundary increases the barrier. This effect disappears with increasing D , and at $D > 10$ the variation of the barrier is less than 2%. Thus, considering a sufficiently deep notch makes it possible to practically avoid the influence of the boundary when studying the influence of the shape and size of the notch on the nucleation barrier. Therefore, we further calculated the nucleation barriers at a fixed notch depth $D = 20$ depending on the radius, which is shown by red in Fig. 2a. The blue dotted line in Fig. 2a shows the radius value above which the barriers of nucleation at a deep notch and at a semicircular notch with the same radius differ by less than 1%. Fig. 2c shows the spin configurations

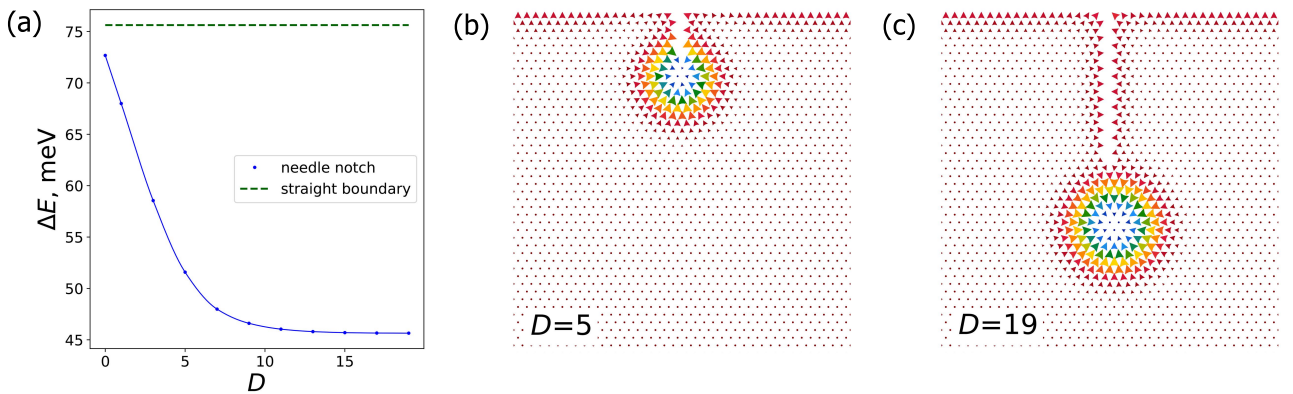


FIG. 4. Energy barrier for skyrmion nucleation at 1-atomic chain notch as a function of notch depth D . Transition states for skyrmion nucleation at the notches with depth $D = 5$ and $D = 19$.

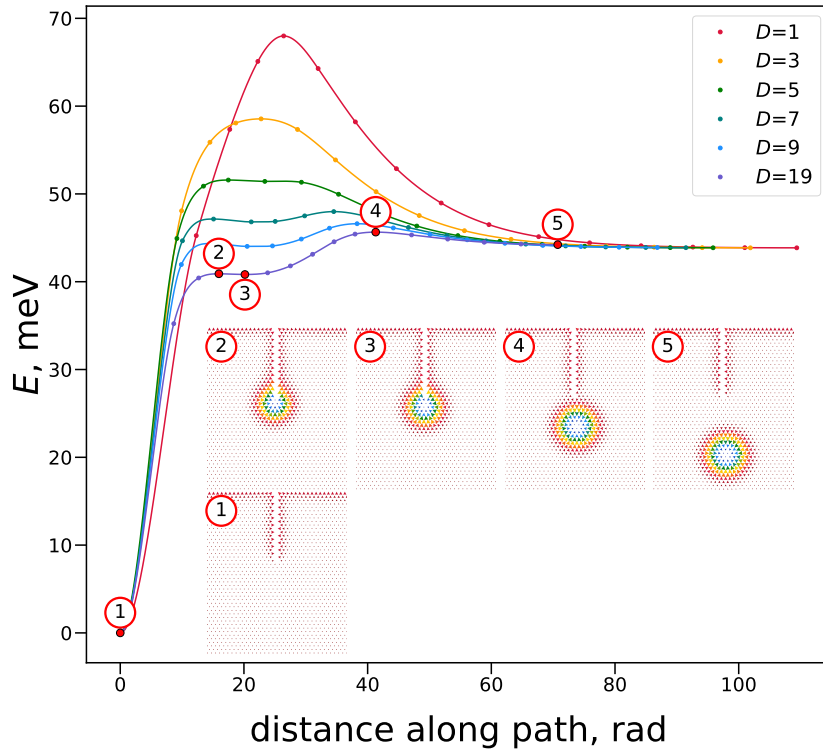


FIG. 5. MEPs for the nucleation of a skyrmion at needle notch of various depth. The insets show magnetic configurations along the MEP for notch depth $D = 19$. States 1, 3, 5 correspond to minima, states 2 and 4 correspond to saddle points.

of saddle points for nucleation on semicircular notches with radii $R = 3$ and 10 , and on notches with depth $D = 20$ and radii $R = 3$ and 10 , and the parameters D and R are indicated. We found that the barrier for nucleation at deep notch decreases down to the narrowest notches. Note that the drop in the barrier when new vacancies appear in the bottom row, discussed above, is qualitatively consistent with this result, since the notch becomes also sharper in that case.

As we have seen, the proximity of the flat boundary and the narrowness of the notch have opposite effects on the barrier of nucleation. The play of these two factors leads to the emergence of a minimum in the region of $R = 4$ for the envelopes shown by dotted curves in Fig. 2a. A minimum of the energy barrier, 58.36 meV, is reached when the notch radius is 4.45 , which is approximately equal to the Sk radius. Qualitatively the same result was obtained in [27]. There, the a skyrmion has been created on a notch by applying an electric current and it was found that skyrmions were born when the curvature radius is comparable to the size of the skyrmion.

Our calculations showed that the smallest barrier in a system with a circular notch is 45.65 meV and is achieved for the narrowest deep notch (smallest R for the red line in Fig. 2a), which corresponds to the needle notch shown in Fig. 4c. To reveal the reason of this result, we plotted the contributions to the energy of the transition state as a function of the notch radius, Fig. 6a, and density of total energy at the transition state, Fig. 6b. The smaller the notch radius, the smaller part of the skyrmion is excluded. As can be seen from Fig. 6b, the notch is located in a region with a negative total energy density. Therefore a narrower notch will lead to a decrease in the energy of the transition state. Fig. 6a shows that all contributions except for DMI one increase as curvature of notch decreases. Therefore the small activation barrier for the sharpest notch is attributed solely to DMI.

Triangular notch. Another basic situation that we studied was nucleation on a triangular shaped notch, Fig. 7b and c show the spin configurations for angles of 30° and 90° . To avoid the influence of a flat boundary, we chose a notch with a depth of $D = 20$, which in this case sets the height of the triangular notch. Fig. 7a shows the calculated dependence of the nucleation barriers on the notch angle. We see that the barrier decreases monotonically with decreasing angle, and the lowest value is achieved at zero angle, which again corresponds to the situation of the needle notch.

In both cases of triangular and round notches, Sk generation is easier for sharper notches. For all studied MEPs transition state (TS) is very similar to the equilibrium Sk touching the tip of the notch. The energy of TS is mainly affected by spins belonging both to the boundary of the track and to the TS. The number of the spins is determined by the “exit length”, to which a measure of effective angle can be attributed, that is, the angle of the triangular notch at which the same barrier value is obtained. Having the dependencies of the energy barrier on the radius of a deep circular notch

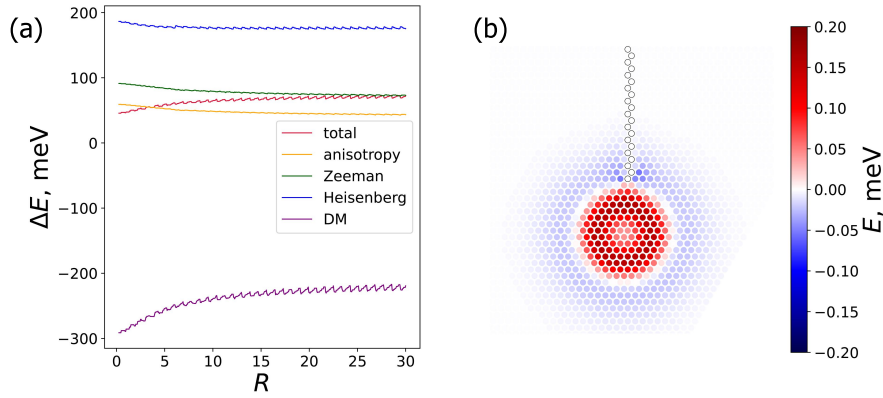


FIG. 6. (a) Contributions of Heisenberg exchange, DMI, anisotropy and Zeeman term to energy of the transition state as function of the round notch radius R for depth $D = 20$. (b) Density of total energy at transition state calculated relatively energy of state without skyrmion.

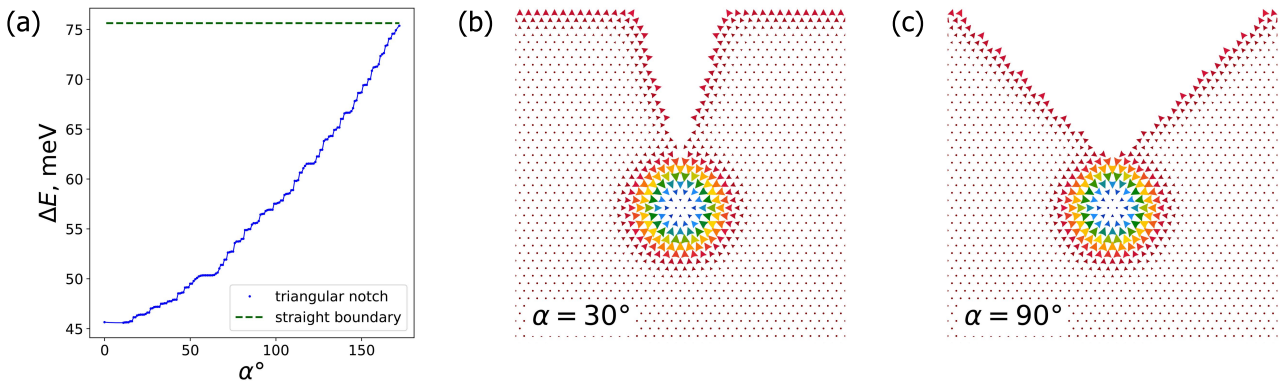


FIG. 7. (a) Energy barrier for skyrmion nucleation at triangular notch as a function of the angle of notch. Transition states for skyrmion nucleation at the notches with angle $\alpha = 30^\circ$ (b) and $\alpha = 90^\circ$ (c).

and on the angle for a triangular notch, we mapped the angle to the radius corresponding the same energy, which gives the effective angle as a function of the radius, Fig. 8. Due to discrete nature of the lattice, precise value of the angle is not strictly defined, thus an interval of angles corresponds to every notch radius. For small radii the effective angle is proportional to the radius:

$$\alpha_{eff} \sim R.$$

For large radii the effective angle dependence on the notch radius is less than variation of the angle due to discreteness of the boundary.

The obtained above results for round and triangular notches allow to estimate activation energy of Sk creation on arbitrary shaped notch. Indeed, an arbitrary boundary can be decomposed to a number of smooth curves connected at non zero angles. The activation barrier for every corner can be estimated by the barrier of the triangular notch having the same angle. The smooth curves are defined by their curvature. As we have seen above, the smallest energy barrier corresponds to the lowest radius of curvature. Hence the activation barrier for a curve can be estimated by the barrier for round notch with the radius equals to the minimum radius of curvature of the curve. The minimal of the barriers of the curves and the corners gives an approximation for the barrier of the corresponding notch.

4. Discussion.

We studied the nucleation of skyrmions on a semicircular notch with the center located at boundary of track, which was previously considered in [27]. It was found that skyrmions are best produced when the notch has a radius that matches the radius of the skyrmion, which is consistent with the results of the work [27]. The barrier depends not only on the radius, but also on the distance to the flat boundary. If we remove the influence of the boundary, the barrier will be determined entirely by the narrowness of the notch. However, if the notch tip is close to the boundary, the energy barrier is larger. So, two factors contribute to the barrier: the value of the radius of the notch, and the proximity to the flat boundary.

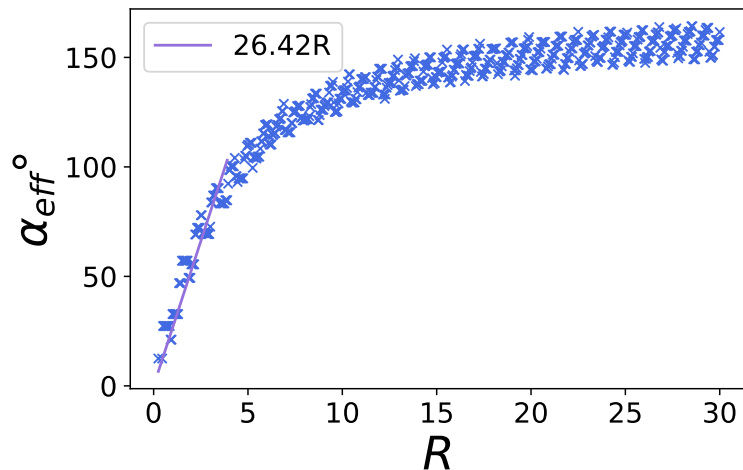


FIG. 8. Correspondence of the radius of a round notch with depth $D = 20$ to the effective angle of triangular notch giving the same nucleation barrier.

Their sum gives the minimum of barrier, or in other words, the most effective Sk generation, that was also observed in the article [27].

For rectangular notch the authors of [27] found that the angle of notch corner 90° is most suitable for the Sk creation, which in contrast to our finding that the best case for creation is the sharpest angle. The reason for that disagreement may be the following. Our calculations showed that the most energetically favorable direction of skyrmion motion during nucleation is along the bisector of notch angle. In the work [27], the direction of movement was different due to the action of the current and perhaps this led to the increase of current density in case of sharpest notches. The current add energy to the system and it can thereby overcome the energy barrier for nucleation, and eventually a skyrmion will appear. We estimated the magnitude of the barrier from which one can obtain an estimate for the minimum current required for nucleation. However, the orientation of the angle notch relative to the direction of the current constrains possible variations of the magnetic moments, therefore the actual magnitude of the current required for nucleation can be higher, which is not taken into account in our approach.

In this work, we did not consider the issue of skyrmion annihilation at the notch. The barrier for annihilation can be found as the difference between the nucleation barrier and the free skyrmion energy calculated relative to the ferromagnetic state. The latest does not depend on the geometry of the sample. Therefore, the behavior of the dependencies of annihilation barriers on geometry qualitatively coincides with the behavior of nucleation barriers presented in this work. The mechanism of skyrmion annihilation on a circular notch of two different radii was considered in the work [30]. It was found that a smaller barrier was obtained with a smaller notch radius, under condition the size of the notch exceeded the size of the skyrmion, which qualitatively coincides with our results.

Previous studies of skyrmion nucleation on a track [20] allow us to compare the results for a track with a straight boundary and with a notch. The barriers for nucleation inside the track and at its boundary were 85.07 meV and 75.62 meV, respectively, while the minimum barrier at the semicircular notch is 58.37 meV, and the barrier at the needle-type notch is 45.65 meV. Thus, for this system, the use of a notch allows one to reduce the barrier of nucleation by up to 50% compared to a track with straight boundaries. Thus, using track notches to create skyrmions could make the process of recording information in memory devices more energy efficient.

Our results allow us to make recommendation for notch design in systems where they are used for positioning Sk. Since energy barriers increase with increasing radius or angle of the notch, for these purposes it is better to use the notch with the largest radii or angles to avoid unwanted creation or destruction of Sk.

In this work, we showed that the Sk nucleation barrier depends both on the local characteristics at the tip of the notch and on the sharpness (radius or angle) of the notch. Also, if the notch is shallow, the barrier will increase due to the proximity of the straight border on either side of the notch. Our calculations provide guidance for creating skyrmions in racetrack memory, namely to use a notch as narrow as possible and with sufficient depth to avoid the influence of flat boundaries.

References

- [1] Parkin S. S. P., Hayashi M., Thomas L. Magnetic domain-wall racetrack memory. *Science*, 2008, **320**, P. 190–194.
- [2] Parkin S. S. P., Yang S.-H. Memory on the racetrack. *Nat. Nanotechnol.*, 2015, **10**, P. 195–198.
- [3] Tomasello R., Martinez E., Zivieri R., et al. A strategy for the design of skyrmion racetrack memories. *Sci. Rep.*, 2014, **4**, 6784.
- [4] Kang W., Huang Y., Zhang X., et al. Skyrmion-electronics: an overview and outlook. *Proceedings of the IEEE*, 2016, **104**(10), P. 2040–2061.

- [5] Stier M., Strobel R., Krause S., et al. Role of impurity clusters for the current-driven motion of magnetic skyrmions. *Phys. Rev. B*, 2021, **103**, P. 054420.
- [6] Zhu H., Xiang G., Feng Y., et al. Dynamics of elliptical magnetic skyrmion in defective racetrack. *Nanomater.*, 2024, **14**(3), P. 312.
- [7] Potkina M.N., Lobanov I.S., Uzdin V.M. Nonmagnetic impurities in skyrmion racetrack memory. *Nanosystems: phys., chem., math.*, 2020, **11** (6), P. 628–635.
- [8] Reichhardt C., Reichhardt C. J. O., Milosevic M. V. Statics and dynamics of skyrmions interacting with disorder and nanostructures. *Rev. Mod. Phys.*, 2022, **94**, P. 035005.
- [9] Boulle O., Vogel J., Yang H., et al. Room-temperature chiral magnetic skyrmions in ultrathin magnetic nanostructures. *Nat. Nanotechnol.*, 2016, **11**, P. 449–454.
- [10] Heinze S., von Bergmann K., Menzel M., et al. Spontaneous atomic-scale magnetic skyrmion lattice in two dimensions. *Nat. Phys.*, 2011, **7**, P. 713–718.
- [11] Bessarab P. F., Müller G. P., Lobanov I. S., et al. Lifetime of racetrack skyrmions. *Sci. Rep.*, 2018, **8**, P. 3433.
- [12] Hagemeyer J., Romming N., Bergmann K. V., Vedmedenko E. Y., Wiesendanger R. Stability of single skyrmionic bits. *Nat. Commun.*, 2015, **6**, P. 8455.
- [13] Koshibae W., Nagaosa N. Creation of skyrmions and antiskyrmions by local heating. *Nat. Commun.*, 2014, **8**, P. 5148.
- [14] Zhou Y., Iacocca E., Awad A. A., et al. Dynamically stabilized magnetic skyrmions. *Nat. Commun.*, 2015, **6**, 8193.
- [15] Romming N., Hanneken C., Menzel M., et al. Writing and deleting single magnetic skyrmions. *Science*, 2013, **341**, P. 636–639.
- [16] Sampaio J., Cros V., Rohart S., Thiaville A., Fert A. Nucleation, stability and current-induced motion of isolated magnetic skyrmions in nanostructures. *Nat. Nanotechnol.*, 2013, **8**, P. 839–844.
- [17] Jiang W., Upadhyaya P., Zhang W., et al. Blowing magnetic skyrmion bubbles. *Science*, 2015, **349**, P. 283–286.
- [18] Uzdin V.M., Potkina M.N., Lobanov I.S., Bessarab P.F., Jónsson H. The effect of confinement and defects on the thermal stability of skyrmions. *Physica B: Condensed Matter*, 2018, **549**, P. 6–9.
- [19] Potkina M.N., Lobanov I.S., Uzdin V.M. Fine energy structure of a magnetic skyrmion localized on a nonmagnetic impurity in an external magnetic field. *Physics of Complex Systems*, 2020, **1** (4), P. 165–168.
- [20] Uzdin V.M., Potkina M.N., Lobanov I.S., Bessarab P.F., Jónsson H. Energy surface and lifetime of magnetic skyrmions. *J. Magn. Magn. Mater.*, 2018, **459**, P. 236–240.
- [21] Hanneken C., Kubetzka A., von Bergmann K., Wiesendanger R. Pinning and movement of individual nanoscale magnetic skyrmions via defects. *New J. Phys.*, 2016, **18**(5), P. 055009.
- [22] Potkina M. N., Lobanov I. S., Uzdin V. M. Nucleation and collapse of magnetic topological solitons in external magnetic field. *Nanosystems: Phys. Chem. Math.*, 2023, **14** (2), P. 216.
- [23] Wang W., Song D., Wei W., et al. Electrical manipulation of skyrmions in a chiral magnet. *Nat. Commun.*, 2022, **13**, 1593.
- [24] Yu X. Z., Morikawa D., Nakajima K., Shibata K., Kanazawa N., Arima T., Nagaosa N., Tokura Y. Motion tracking of 80-nm-size skyrmions upon directional current injections. *Sci. Adv.*, 2020, **6**, eaa9744.
- [25] Twitchett-Harrison A. C., Loudon J. C., Pepper R. A., Birch M. T., Fangohr H., Midgley P. A., Balakrishnan G., Hatton P. D. Confinement of skyrmions in nanoscale FeGe device-like structures. *ACS Appl. Electron. Mater.*, 2022, **4** (9), P. 4427–4437.
- [26] Büttner F., Lemesh I., Schneider M., et al. Field-free deterministic ultrafast creation of magnetic skyrmions by spin–orbit torques. *Nature Nanotech.* 2017, **12**, P. 1040–1044.
- [27] Iwasaki J., Mochizuki M., Nagaosa N. Current-induced skyrmion dynamics in constricted geometries. *Nature Nanotech.*, 2013, **8**, P. 742–747.
- [28] Koshibae W., Kaneko Y., Iwasaki J., Kawasaki M., Tokura Y., Nagaosa N. Memory functions of magnetic skyrmions. *Jpn J. Appl. Phys.*, 2015, **54**, P. 053001.
- [29] Behera A. K., Murapaka C., Mallick S., Singh B. B., Bedanta S. Skyrmion racetrack memory with an antidot. *J. Phys. D: Appl. Phys.*, 2021, **54**, P. 025001.
- [30] Suess D., Vogler C., Brückner F., Heistracher P., Slanovc F., Abert C. Spin torque efficiency and analytic error rate estimates of skyrmion. *Sci. Rep.*, 2019, **9**, P. 4827.
- [31] Dutta S., Nikonov D. E., Bourianoff G., Manipatruni S., Young I. A., Naeemi A. Skyrmion nucleation via localized spin current injection in confined nanowire geometry in low chirality magnetic materials. 2018. arXiv: 10.48550/arXiv.1801.10525.
- [32] Xu M., Zhang J., Meng D., Zhang Z., Jiang G. The influence of introducing holes on the generation of skyrmions in nanofilms. *Phys. Lett. A.*, 2022, **433**, P. 128034.
- [33] Fert A., Cros V., Sampaio J. Skyrmions on the track. *Nat. Nanotechnol.*, 2013, **8** (3), 152.
- [34] Jiang W., Zhang W.; Yu G., et al. Mobile Néel skyrmions at room temperature: status and future. *AIP Advances*, 2016, **6**, P. 055602.
- [35] Kang W., Huang Y., Zheng C. et al. Voltage controlled magnetic skyrmion motion for racetrack memory. *Sci Rep*, 2016, **6**, 23164. <https://doi.org/10.1038/srep23164>
- [36] Morshed M. G., Vakili H., Ghosh A. W. Positional stability of skyrmions in a racetrack memory with notched geometry. *Phys. Rev. Applied*, 2022, **17**, P. 064019.
- [37] Belrhazi H., El Hafidi M. Nucleation and manipulation of single skyrmions using spin-polarized currents in antiferromagnetic skyrmion-based racetrack memories. *Sci. Rep.*, 2022, **12**, 15225.
- [38] Weinan E., Ren W., Vanden-Eijnden E. String method for the study of rare events. *Phys. Rev. B*, 2002, **66**, P. 052301.

Submitted 25 February 2024; revised 13 April 2024; accepted 14 April 2024

Information about the authors:

Maria N. Potkina – Infochemistry Scientific Center, ITMO University, 197101 St. Petersburg, Russia; ORCID 0000-0002-1380-2454; potkina.maria@yandex.ru

Igor S. Lobanov – Faculty of Physics, ITMO University, 197101 St. Petersburg, Russia; ORCID 0000-0001-8789-3267; lobanov.igor@gmail.com

Conflict of interest: the authors declare no conflict of interest.